

Research Article

A Low-Cost Closed-Loop Solar Tracking System Based on the Sun Position Algorithm

Muhammad E. H. Chowdhury,¹ Amith Khandakar ¹, Belayat Hossain ²,
and Rayaana Abouhasera¹

¹Electrical Engineering Department, College of Engineering, Qatar University, Doha 2713, Qatar

²Department of EECS, Graduate School of Engineering, University of Hyogo, Kobe, Japan

Correspondence should be addressed to Belayat Hossain; belayat@ieee.org

Received 3 December 2018; Revised 22 January 2019; Accepted 4 February 2019; Published 27 February 2019

Academic Editor: Antonio Lazaro

Copyright © 2019 Muhammad E. H. Chowdhury et al. This is an open access article distributed under the Creative Commons Attribution License, which permits unrestricted use, distribution, and reproduction in any medium, provided the original work is properly cited. The publication of this article was funded by Qatar National Library.

Sun position and the optimum inclination of a solar panel to the sun vary over time throughout the day. A simple but accurate solar position measurement system is essential for maximizing the output power from a solar panel in order to increase the panel efficiency while minimizing the system cost. Solar position can be measured either by a sensor (active/passive) or through the sun position monitoring algorithm. Sensor-based sun position measuring systems fail to measure the solar position in a cloudy or intermittent day, and they require precise installation and periodic calibrations. In contrast, the sun position algorithms use mathematical formula or astronomical data to obtain the station of the sun at a particular geographical location and time. A standalone low-cost but high-precision dual-axis closed-loop sun-tracking system using the sun position algorithm was implemented in an 8-bit microcontroller platform. The *Astronomical Almanac's* (AA) algorithm was used for its simplicity, reliability, and fast computation capability of the solar position. Results revealed that incorporation of the sun position algorithm into a solar tracking system helps in outperforming the fixed system and optical tracking system by 13.9% and 2.1%, respectively. In summary, even for a small-scale solar tracking system, the algorithm-based closed-loop dual-axis tracking system can increase overall system efficiency.

1. Introduction

With the rapid growth of population and economic development, there is an increasing concern due to the energy crisis and environmental pollution; researchers are trying to explore new technologies for the production of electricity from clean and renewable sources such as solar and wind. Solar energy is one of the primary sources of clean, abundant, and inexhaustible energy that not only provides alternative energy resources but also improves environmental pollution. Moreover, the accessibility of this energy is significantly higher in a subtropical country, like Qatar. Annual Direct Normal Irradiance (DNI) of 1800 kWh/m²/y is enough for concentrated solar power plants, where Qatar has DNI value of 2008 kWh/m²/y. DNI between the range of 2000 to 2800 kWh/m²/y is considered feasible [1]. Thus, Qatar has a huge potential for harnessing the solar energy via a solar

photovoltaic (PV) power plant. It is possible to convert solar energy into mechanical energy or electricity with adequate efficiency. Information about the quality and amount of solar energy available at a specific location is of prime importance for the development of a solar energy system. However, the amount of electricity that is obtained is directly proportional to the intensity of sunlight falling on the photovoltaic panel.

To get a larger amount of solar energy, the efficiency of photovoltaic systems has been studied by a large number of scientists and engineers. In general, there are three ways to increase the efficiency of photovoltaic systems [2]. The first method is to increase the efficiency of power generation of the solar cells, the second is related to the efficiency of the control algorithms for the energy conversion, and the third approach is to adopt a tracking system to achieve maximum solar energy. The focus area of this paper is to increase efficiency by combining the second and third approaches.

Several solar controlling and tracking systems are proposed in the literature; one can classify them according to their degrees of freedom (DoFs) and/or control strategy. Regarding DoF, there are three main types of trackers [3]: fixed devices [4], single-axis trackers [5], and dual-axis trackers [6]. Different researchers have reported the potential system benefits of using a simple single-axis tracking solar system [7, 8]. The data acquisition, control, and monitor of the mechanical movement of the photovoltaic module were implemented based on a programmable logic-controlling unit. Some researchers [9–15] also present the design and construction of a two-axis solar tracking system in order to track the photovoltaic solar panel according to the direction of beam propagation of solar radiation. To achieve maximum solar energy, solar power systems generally are equipped with devices, which are calculating the maximum power point tracking (MPPT) [16–19].

Regarding the control strategy, three main types of solar trackers exist: passive, open-loop, and closed-loop controlled trackers. The passive trackers have no electronic sensors or actuators, but rather, various properties of matters (thermal expansion, pressure control, or other mechanical arrangements) have been used for the solar position prediction [20, 21]. The passive sensor-based solar positioning system does not measure the solar position accurately, although they are reliable and simple in design due to exclusion of any electronic control or motors and are almost maintenance-free [20]. However, the system is not able to track the temperature variability that happens from one day to another. In addition, the system can lead to unpredictable movement due to the mechanics. Such unpredictable movement happens especially on overcast days, when the sun is visible and invisible due to the clouds or when the sun is randomly covered by clouds. Moreover, real-time implementation of the solar positioning system accurately is difficult due to the calibration required for the smooth operation of the system. The open-loop ones have no sensors either but use a microprocessor and are based on the sun position algorithm using a mathematical formula to obtain the station of the sun at a particular location and time, and it does not need to sense any physical quantity [22–24]. The third kind of trackers uses the information of electrooptic sensors [25–29] (auxiliary bifacial solar cell panel, charge-coupled device (CCD) camera, photocell, light-dependent resistors, etc.). These systems are popular as these have positive effect on increasing efficiency in sunny days. However, these systems fail to measure the solar position in a cloudy day or intermittent sunny day. Such systems are complex due to the usage of different and/or numerous sensors. Moreover, it requires a very precise installation. An open-loop type of controller does not observe the output of the processes that it is controlling. Consequently, an open-loop system cannot correct any errors and thus may not compensate for disturbances in the system. The system is simpler and cheaper than the closed-loop type of sun-tracking systems [30]. In the open-loop mode, the computer or a processor calculates the sun's position from the formula or algorithms using its time/date and geographical information to send signals to the electromotor. However, in some cases, many sensors are used to identify

specific positions [31, 32]. Among the many works done in the design and implementation of a low-cost dual-axis autonomous solar tracker, recently, Gabe et al. have worked on designing a complete autonomous solar tracker [33] which is an example of a closed-loop controlled tracker using light-dependent resistors (LDRs) and has the same issues which are discussed earlier.

A good number of real-time solar position measurement algorithms have been developed (sun position algorithm (SPA) [34], *Astronomical Almanac's* (AA) [35], and Roberto Grena's Energy and Sustainable Economic Development (ENEA) [36]) which are more accurate to measure the solar position than the sensor-based solar positioning system. Several researchers [37, 38] have implemented the sun position algorithm to detect the sun position accurately in a microprocessor and personal computer platform. These algorithms are mainly developed for locating the sun position using a standard microprocessor-based system which is not standalone and not applicable in remote areas due to power and management requirements. It is difficult to implement standard algorithms in the standalone electronic control system due to computation complexity of the sun position algorithms, which could offer highly reliable real-time sun position information without much increasing system cost and avoiding the requirement of time-to-time calibration.

A solar position system that can work standalone without the necessity of being developed in a powerful microprocessor with the standard solar positioning algorithm used for positioning is worthwhile. In this work, a simple, cost-effective algorithm-based reliable two-axis tracking system has been developed for real-time solar position measurement on an 8-bit microcontroller platform. Firstly, a comparative MATLAB-based (The MathWorks, Natick, MA) simulation study was carried out between three popular solar position algorithms: SPA, AA, and ENEA. Secondly, the most feasible and relatively accurate algorithm was implemented in an 8-bit microcontroller to compare its performance in comparison to simulation. Thirdly, three different tracking systems, fixed orientation PV solar panel, four light-dependent resistor- (LDR-) based optical sensor, and AA algorithm-based dual-axis closed-loop solar tracker, were designed and implemented in an 8-bit microcontroller platform. Finally, the dual-axis solar tracker's performance was compared with the fixed orientation PV solar panel and optical solar tracking system. The prototyped system was evaluated with the MATLAB-based simulated results and real-time sun position results from the prototype system.

This paper is organized into sections. Section 2 is describing the system materials and methods along with the comparisons between the proposed and popular sun position algorithms. Section 3 shows the comparisons of outcomes between the fixed orientation PV solar panel and optical solar tracking system with the proposed solution, and finally, the conclusion is drawn in Section 4.

2. Materials and Methods

2.1. System Block Diagram. The main elements of a typical solar tracking system are the sun-tracking system, control

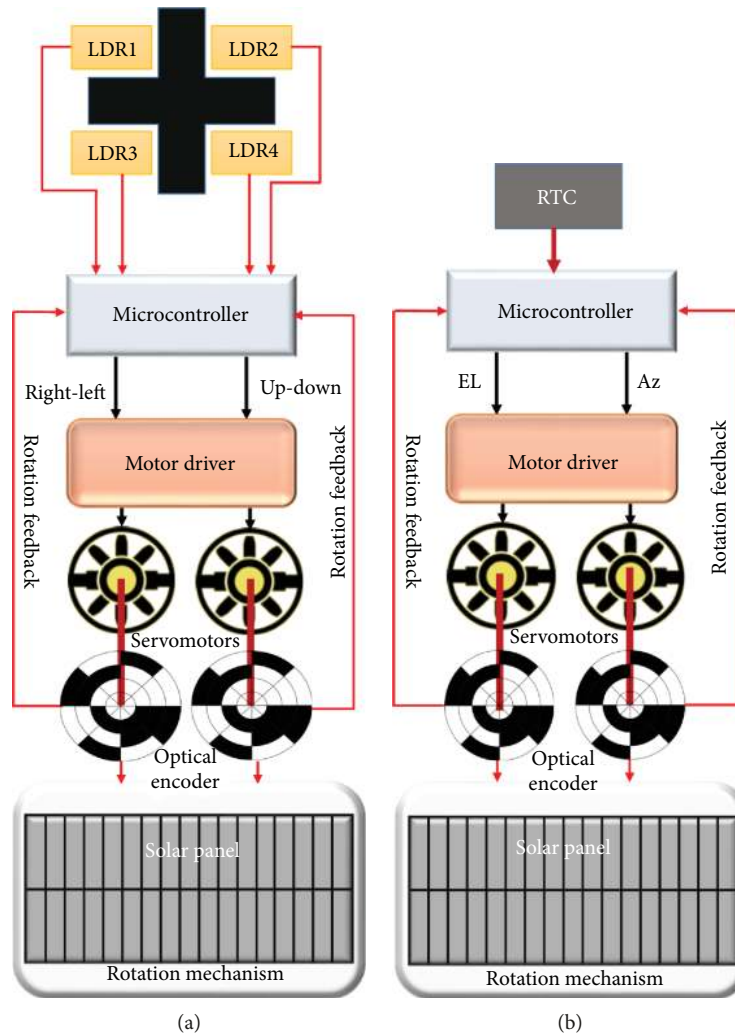


FIGURE 1: System block diagram: (a) using optical tracking and (b) proposed sun position algorithm-based tracking.

unit, positioning system, drive mechanism, and sensing devices. The system architecture of the optical sensor-based and proposed systems is shown in Figure 1. The main difference in both systems is that the first one requires a signal conditioning circuit and LDR sensors; however, the latter one does not need any sensor except a real-time clock (RTC) to input real-time to the algorithm. The system block was implemented in the ATmega328P microcontroller along with the Arduino development board. The ATmega328 is a single-chip microcontroller created by Atmel (known as Microchip Technology now). It has a modified Harvard architecture 8-bit (reduced instruction set computer) RISC processor core. ATmega328P, in 28-pin narrow dual in-line package (DIP-28N) version, was used in the implementation. Arduino integrated development environment (IDE) v1.6.12 in the Windows platform was used to compile the code written in C++ language. The compiled program was uploaded on the Arduino UNO, an open-source microcontroller board based on the Microchip ATmega328P microcontroller and developed by Arduino.cc. It was uploaded on the ATmega328P with the Arduino IDE via a type B USB cable. The motor controllers were implemented in the Arduino motor

shield. The tracker has two degrees of freedom, which is required to track the solar position using its azimuthal and elevation angles.

The PDV-P8001 photoresistors (made from cadmium sulfide (CdS)) from Adafruit were used in this work. The diameter of the LDRs is 5 mm, while the height is 2.09 mm. The LDRs are placed at the top of the centre of the solar panel in the arrangement shown in Figure 1. The horizontal separation between the LDRs 1 and 2 and LDRs 3 and 4 is 5 mm, whereas the diagonal separation between LDRs 1 and 4 and LDRs 2 and 3 is 10 mm. The solar panel was a small uxcell polycrystalline solar panel (6 V, 120 mA, and 0.65 W) to proof the concept of the tracker. The YMT22 Optical Encoder hollow shaft incremental motor servomotor encoder was used with the FS5106R FEETECH Continuous Rotation Servo. Figure 2 summarizes the components used in this work.

The basic operation of the systems is described as follows. The microcontroller sends signals (as pulse width modulation (PWM)) to the servomotors, which have integrated gears and a shaft that can be controlled. Two servomotors are for rotating the solar panel about the horizontal and







Exp. no	Features	Details	Image
FS5106R FEETECH Continuous Rotation Servo	Speed @ 6 V	95 rpm	
	Stall torque @ 6 V	83 oz-in	
PDV-P8001 photoresistors	Size	Round, 5 mm (0.2") diameter and 2.09 mm height.	
	Resistance range	200KΩ (dark) to 10KΩ (10 lux brightness)	
	Sensitivity range	CdS cells respond to light between 400 nm (violet) and 600 nm (orange) wavelengths, peaking at about 520 nm (green).	
Uxcell Poly Mini Solar Panel	Technical specification	6 V, 120 mA, and 0.65 W	
	Dimension	120 × 56 mm/4.72" × 2.2" (L*W)	
	Thickness	2.5 mm/0.1 inch	
YMT22 Optical Encoder	Supply voltage	DC5V (±10%)	
	Max. response frequency	30 Hz	
	Resolution	Up to 300 pulse per rotation (ppr)	
	Max. rotation speed	3000 revolution per minute (rpm)	
DS3231 Real-Time Clock Module Board	Real-time clock	Counts seconds, minutes, hours, date of the month, month, day of the week, and year with leap year (up to 2100)	
	Serial I/O	I ² C communication	
	Supply voltage	2.0 V to 5.5 V (battery back-up)	
Arduino Sensor Shield	Interface	Analogue pins A0 to A5, I2C, serial	
	Connectable modules	Sensor modules, servo's, or I2C LCD	

FIGURE 2: List of the major components with their basic features.

vertical axes so that it can move the solar panel toward the sun. The microcontroller calculates the sun position from the algorithm using the geographical location, time, and date (using a DS1302 real-time clock (RTC) module) as shown in Figure 1(b). Elevation and azimuth angles were calculated, and the microcontroller commanded the servomotors to the desired angles. Optical encoders were attached to the shaft of each motor so that the amount of rotation accomplished by each motor can be tracked, and if any deviation occurred, the controller would fix that.

2.2. Sun Position Algorithms. The sun position algorithms calculate the solar azimuth (φ) and elevation (EL) (e) angles of the sun. These angles are then used to position the solar panel toward the sun. The zenith angle (θ) is the angle between the direction of the sun (direction of interest) and the zenith (straight up or directly overhead). The sun elevation or altitude (e) is the angle from the horizontal plane

and the sun's central ray or just the complement of the zenith angle (90° -zenith angle). The azimuth angle (Az) (ϕ) is measured clockwise from true north to the point on the horizon directly below the object.

Figure 3 depicts the parameters associated with the sun position measurement. The elevation angle (e) is calculated using any one of the following formulas (depending on the algorithm such as $eSPA$ is the elevation angle calculated using the SPA, eAA is the elevation angle calculated using the AA algorithm, and $eENEA$ is the elevation angle calculated using the ENEA algorithm):

$$\begin{aligned}
 eSPA &= a \sin \left(\sin \varphi \sin \delta_t + \cos \varphi \cos \delta_t \cos h'_a \right), \\
 eAA &= a \sin \left(\sin \varphi \sin \delta + \cos \varphi \cos \delta \cos h_a \right), \\
 eENEA &= a \sin \left(\sin \varphi \sin \delta_t + \cos \varphi \cos \delta_t \cos h_t \right),
 \end{aligned} \tag{1}$$

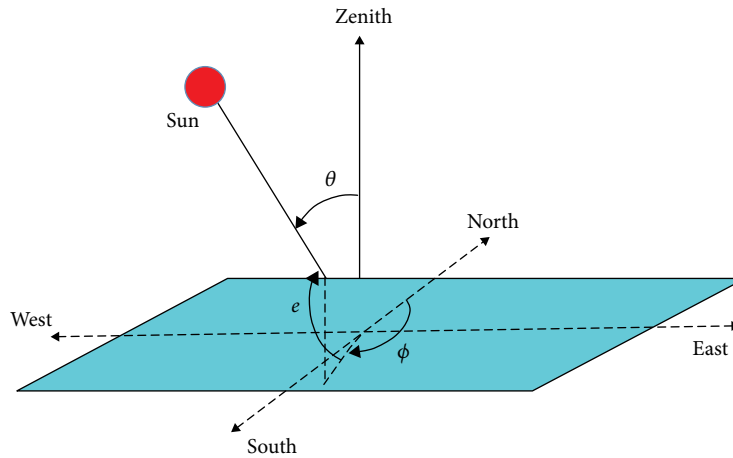


FIGURE 3: Parameters of the solar position algorithm.

and the azimuthal angle is calculated by any algorithm (such as Φ_{SPA} is the azimuthal angle calculated using the SPA, Φ_{AA} is the azimuthal angle calculated using the AA algorithm, and Φ_{ENEA} is the azimuthal angle calculated using the ENEA algorithm) as follows:

$$\begin{aligned} \Phi_{SPA} &= a \tan 2 \left(\frac{\cos h'_a}{\cos h'_a \sin \varphi - \tan \delta_t \cos \varphi} \right), \\ \Phi_{AA} &= a \sin \left(-\cos \delta \frac{\sin h_a}{\cos e} \right), \\ \Phi_{ENEA} &= a \tan 2 (sh_t, ch_t \sin \varphi - \tan \delta_t \cos \varphi), \end{aligned} \quad (2)$$

where φ is latitude, δ is the declination angle, δ_t is the topocentric declination angle, h_a is the hour angle, h'_a is the topocentric hour angle, and sh_t and ch_t are approximate sine and cosine of the hour angle, respectively.

The comparison of the three algorithms is necessary for feasibility study of the electronic implementation of the algorithms in an 8-bit microcontroller. Therefore, a comparative simulation study, in terms of both implementation complexity and computational cost, of those algorithms was carried out, and results are described in Section 3.

2.3. Simulation Study. Simulations of the three popular algorithms (SPA, AA, and ENEA) have been carried out in MATLAB (R2015a) [18], and the in-house built MATLAB codes were tested in a Windows machine with Pentium Dual-Core 2.2 GHz CPU, 2 GB RAM, and 64-bit Windows 7 operating system.

MATLAB script for each algorithm (AA, ENEA, and SPA) was tested separately to get the sun position (e and ϕ angle) at three randomly chosen days over the year (March 21, July 10, and December 15, 2016) which represent winter, beginning of summer, and midsummer. The location (lat: 25.37463 and long: 51.49128) of Qatar University (QU) was used for simulation and experimental study. In the AA algorithm, the sun position was calculated for the mentioned dates using date, time, latitude, and longitude as input parameters. However, both ENEA algorithm and SPA require one

additional parameter altitude (31 m) of the location. The absolute difference between the simulated elevation and azimuth angle among each other for ENEA, AA, and SPA was calculated to evaluate the performance of the algorithms. SPA is capable of calculating the solar elevation and azimuth angles in the period from the year -2000 to 6000, with uncertainties of ± 0.0003 , which reflects a very high accuracy [34]. However, the algorithm is a slow algorithm for the computation of the sun position with respect to an observer at the ground surface.

2.4. Experimental Study. The AA algorithm was used in this work for implementation because of its simplicity, reliability, and fast computability of the solar position valid for the long period of time (1950-2050) (with uncertainty of greater than $\pm 0.01^\circ$) [35] compared to another fast algorithm ENEA (valid for only 2003-2022) (with the minimum uncertainty of $\pm 0.002^\circ$) [36]. On the contrary, SPA is very accurate and valid until year 6000 but is a slow algorithm for the computation of the sun position. Moreover, implementation of SPA in an 8-bit microcontroller is not possible because of its complexity whereas the accuracy of AA is comparable to SPA, and AA is well recognized for computing the sun position. Moreover, the AA algorithm has been compared with other standard algorithms (ENEA and SPA) using MATLAB simulation to show the relevance of using AA for implementation.

To evaluate the performance of the algorithms and to decide whether it is worth to implement AA or ENEA algorithms experimentally, the simulated elevation and azimuth angle for the three mentioned dates were plotted against the hours of the day. Figure 4 shows e and ϕ angle for the three algorithms on March 21, July 10, and December 15, 2016, respectively.

2.5. System Implementation. Implementation of the most accurate SPA in an 8-bit microcontroller was not possible because of its complexity whereas AA is also very accurate and well recognized for computing the sun position using mathematical equations, implementable in an 8-bit microcontroller. The "AA algorithm" must be implemented as a

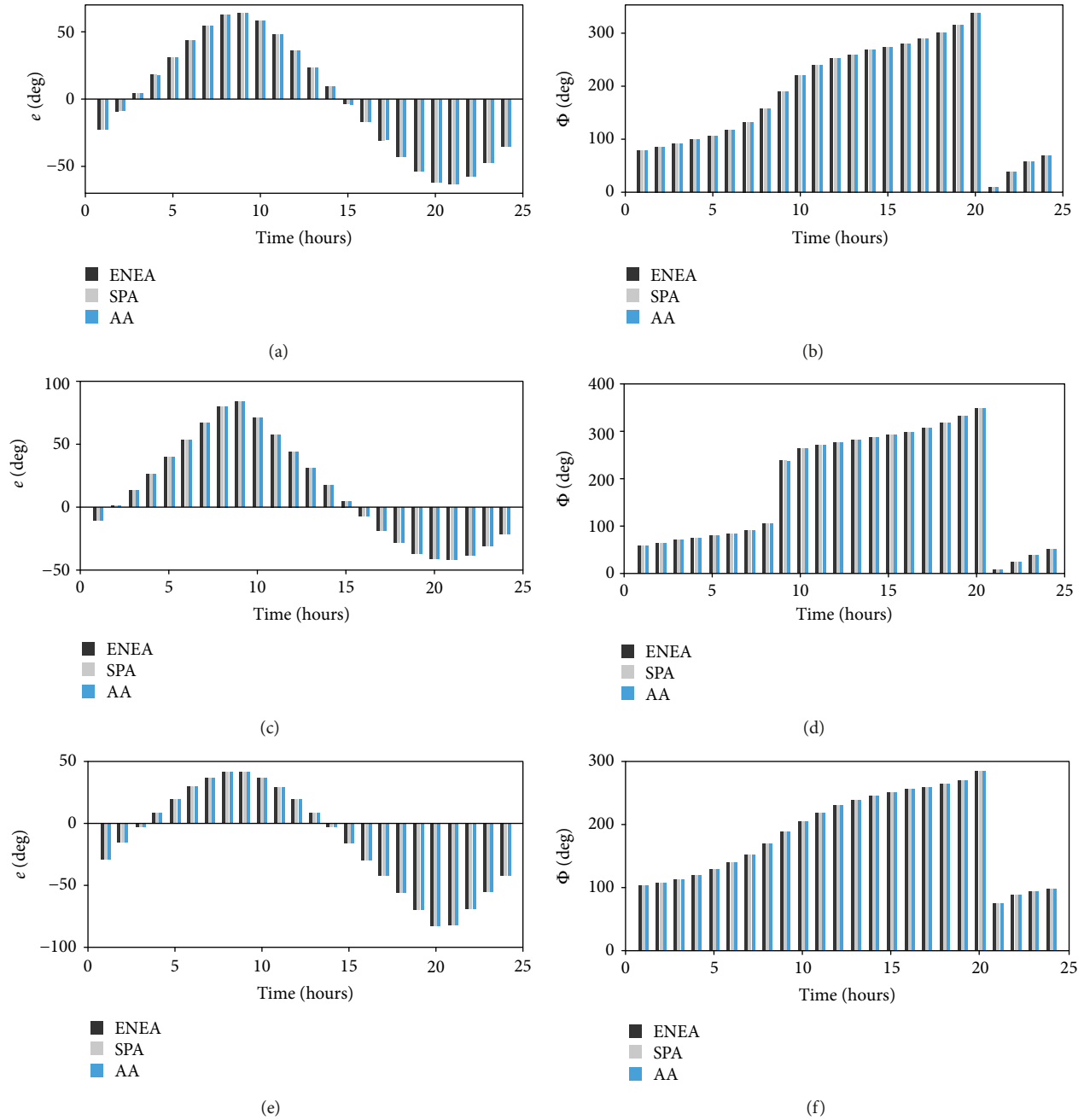


FIGURE 4: Variation of EL and Az angles for simulated results on 21 March, 10 July, and 15 December 2016, respectively, for Qatar. Note that the positive values of the elevation angles represent daytime, whereas the negative angles represent nighttime.

function of the location and time of the specific site where the equipment will be placed. A prototype of the fixed inclination solar panel, closed-loop dual-axis tracking system (as shown in Figure 5(a)) was developed using the conventional optical-based (LDRs) tracking and sun position algorithm-based tracking (Figure 5(b)) to compare the performance of the systems. The optical tracking system is based on four LDRs that will detect the light levels and convert them to voltages which were compared by the microcontroller to determine the brightest region. On the contrary, the location of the sun was calculated using the AA algorithm to find azimuthal (Az) and elevation (EL) angles of the sun

to adjust the orientation of the solar panel. The advantage of using the ATmega328P microcontroller for implementation is that there are several trigonometric functions, which are essential to implement the AA algorithm, which are already available as built-in functions. To compare the tracking-based systems with the fixed system, the solar system was placed at 81° fixed inclinations to the zenith. The voltage measured by the microcontroller onboard 10-bit analog-to-digital converter (ADC) is the open-circuit voltage measured across the PV panel. The photovoltaic (PV) terminals were connected to the ADC input of the microcontroller through a voltage divider network to make sure that the

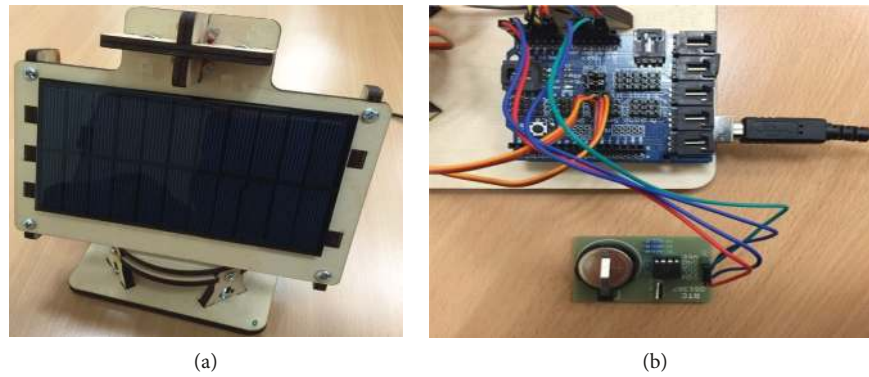


FIGURE 5: Prototype of the solar tracker system (a) and the microcontroller with a sensor shield and RTC (b).

voltage applied at the input of ADC remains smaller than 5 V while the PV panel is producing maximum voltage. This is because the ADC input of the microcontroller can withstand maximum of 5 V. The voltage reading acquired using the microcontroller was compared with the Fluke 117 Electricians True RMS Multimeter, which shows a good agreement between the microcontroller reading and the Fluke meter reading. For further quantification of the performance of the proposed system with respect to contemporary systems, this study calculated the area under the voltage-time curve (AUC) of the panel voltage vs. time graphs obtained from the three systems. AUC was calculated by the trapezoidal rule. It consists in dividing the voltage-time profile into several trapezoids and calculating the AUC by adding the area of these trapezoids. Several experimental data were taken from the three systems which were placed at the same location and time to make sure that all systems are illuminated under the same condition. Each experimental data was acquired in a different day, but operating duration was the same (sunrise to sunset).

3. Results and Discussion

Figure 4 shows that the solar positions simulated at different hours of three different days were very similar. Figure 6 shows that the ENEA algorithm's accuracy is higher than that of the AA algorithm, but the ENEA algorithm will not be valid after 2022. The overall difference in the solar position using AA from SPA is not higher than 0.4° . Since the SPA is computationally expensive and not implementable in a low-speed, low-power-consuming microcontroller, the computationally cost-effective AA algorithm was implemented for the experimental study. The difference between the simulated and experimental values for the elevation and azimuth angles obtained in three individual days was calculated and plotted in Figure 7, where in all cases the difference was less than 0.6° . So, the outcome of the proposed implemented system has almost the same performance compared to the ideal case which was simulated in the computer. This error could be introduced due to the 8-bit implementation of the AA algorithm. Furthermore, the experimental results shown in Figure 8 were recorded from the prototype systems at the same time on an intermittently cloudy day in three scenarios: with the solar system placed at 81° fixed inclinations to the

zenith, with optical tracking, and with solar position-based tracking. The results confirmed that the proposed system outperforms significantly from the fixed solar system and also the conventional optical tracker. Furthermore, the algorithm-based proposed system was more stable than the optical one. The operation of this system is independent of periodic calibration, and it can be made independent of geographical location by adding a Global Positioning System (GPS) receiver in the system.

The panel voltage acquired in a sunny day is shown in Figure 7. However, it is obvious that the uncertainty in the voltage reading of the microcontroller-based voltmeter is 2.44 mV (half of the resolution of the ADC, $5\text{ V}/(2^{10}/2)$). Therefore, the uncertainty in the reading is quite small. Moreover, with the advancement of embedded electronics, it is possible to get a cheap and miniature microcontroller with a higher number of ADC bits which can measure voltage with much higher accuracy. The area under the panel voltage-time curve (AUC) (an example is shown in Figure 8) reflects the actual energy harnessed by the solar panel after positioning the system toward the sun and is expressed in V^*hr . This AUC is dependent on positioning of the tracker toward the sun, time of the operation, and the energy-harnessing capability by the system. The total amount of energy harvested by the system may be assessed by adding up or integrating the amounts eliminated in each time interval, from time zero (time of the initial operation of the system) to infinite time. This total amount corresponds to performance of the tracker in terms of the energy harvested from the sun by the system. The AUC is directly proportional to the incidence of solar radiation falls on the panel. That is, it has high value during noon of a shiny day but zero value at night.

Table 1 shows the AUC values of the three systems which shows that our proposed algorithm-based system (has the highest average AUC value) outperformed over other conventional systems. Therefore, the tacker with the highest average AUC value indicates the best performance in terms of energy harvesting from the sun which indicates the best positioning of the system toward the sun. It is therefore apparent from the table that the algorithm-based tracker outperforms over fixed tracking and optical tracking by 13.9% and 2.1%, respectively. Moreover, the standard deviation calculated over the trials showed that the algorithm-based

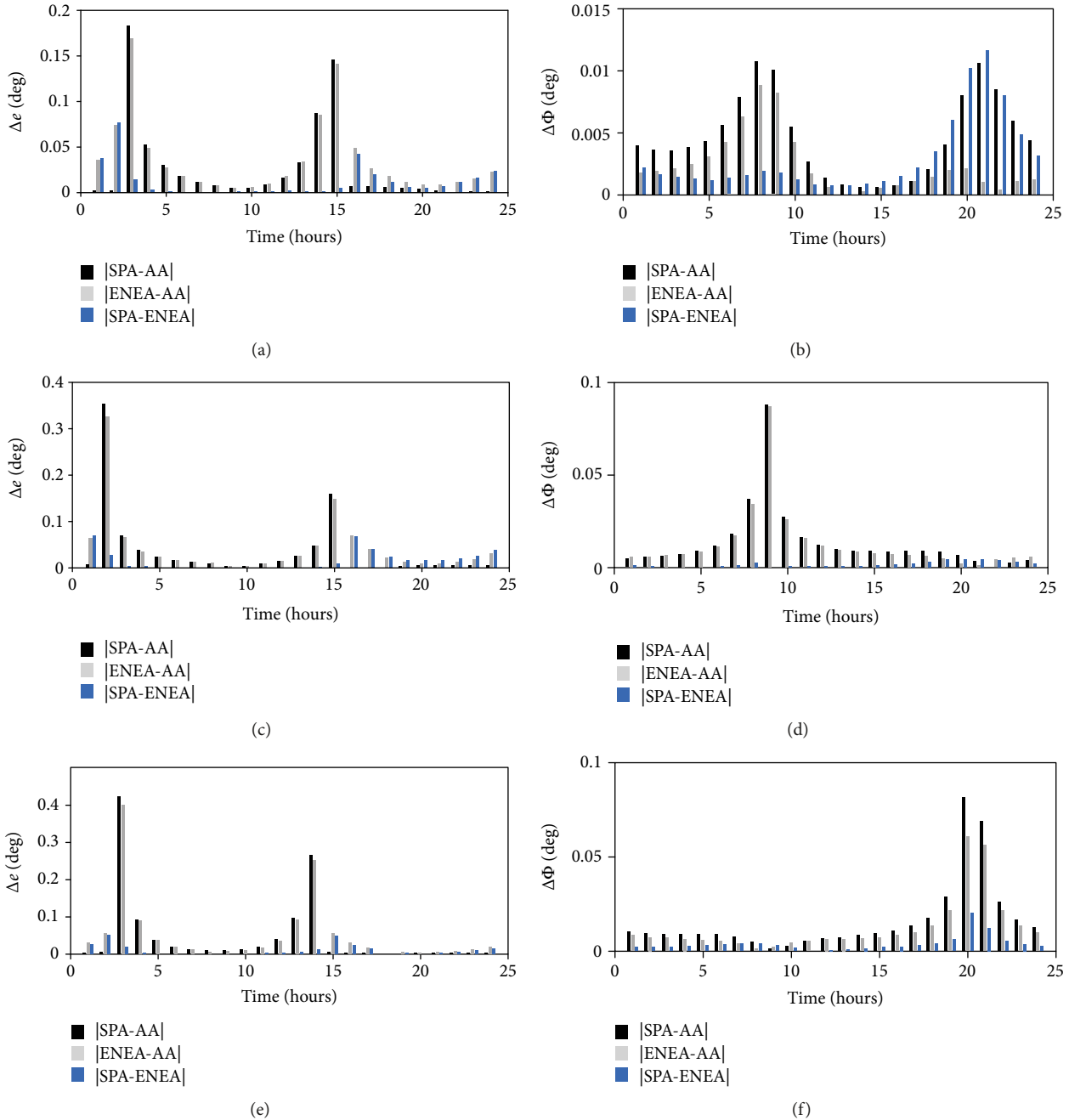


FIGURE 6: Differences of SPA and AA, ENEA and AA, and SPA and ENEA for the variation of EL and Az angles for the simulated results on 21 March, 10 July, and 15 December 2016, respectively, for Qatar.

tracker provide the least variation in the trials, which reflects the highest throughput of the system with stable system response.

4. Conclusions

A real-time solar position tracking system was successfully implemented using the AA algorithm, which is implementable in an 8-bit microcontroller. The additional hardware requirement for identifying the solar position using the AA algorithm is minimum while the solar tracking code was

executed in less than a second, which makes it suitable for real-time application using an 8-bit microcontroller. Moreover, the algorithm is valid till 2050, and therefore, this algorithm will be usable in the next three decades. In order to show the accuracy of the AA algorithm, it was compared to other standard algorithms (ENEA and SPA), where it was proved that the accuracy of the AA algorithm is comparable to other algorithms in measuring the sun position. Moreover, the measured solar panel voltage also reflects that a close-loop algorithm-based dual-axis tracker can be implemented using an 8-bit microcontroller, which outperforms

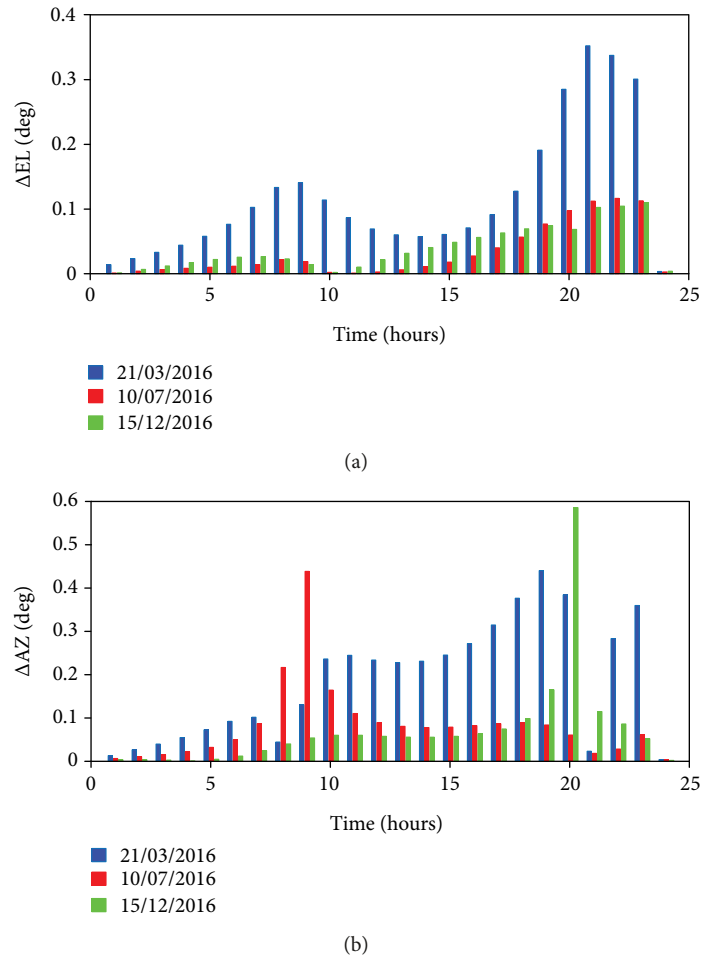


FIGURE 7: Difference of EL and Az between the simulated and experimental results ((experimental–simulated)).

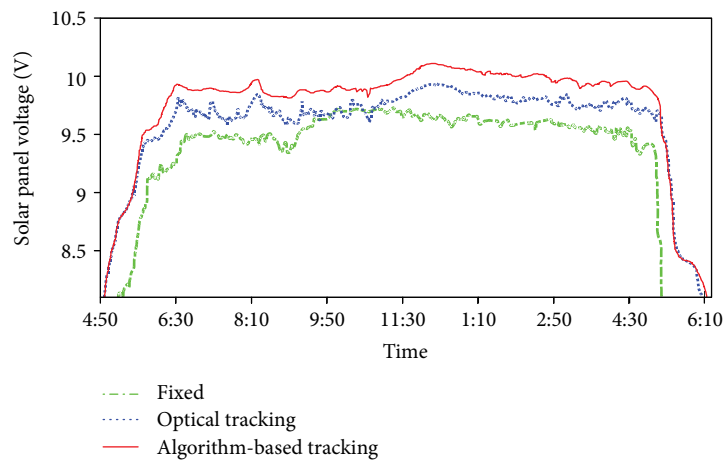


FIGURE 8: An example of panel voltage versus a time graph taken randomly from the experiments. It shows comparison of PV panel voltage generation between dual-axis algorithm-based tracking, optical tracking, and fix-angle systems. Here, the unit of time is hour.

a conventional optical tracker without adding system cost. Other benefits of the proposed system are that it is standalone with high accuracy in tracking the sun position (maximum uncertainty of position detection is 0.6°). In this small-scale

prototype implementation, we did not consider the lead resistance of the photoresistors. For a large full-scale operational system, the designer needs to consider lead resistance for the photoresistors. However, this limitation can be easily

TABLE 1: Comparison among the three sun trackers using the area under the curve.

Exp no.	Fixed tracker	Optical sensor-based	Algorithm-based
1	6899	7661	7820
2	6901	7729	7895
3	7005	7850	7950
4	6950	7801	7918
5	6769	7499	7750
Average/standard deviation	6905/±78	7708/±123	7867/±72

removed by incorporating a wireless photoresistor data transmission system to the main controller using radio frequency (RF) chips (e.g., nRF24L01) or a miniature microcontroller with an embedded Bluetooth module (e.g., RFduino). Therefore, in the small-scale prototype implementation, we did not consider this aspect of the design, which we believe can be minimized easily for large-scale implementation. In the future, the proposed electronic implantation of the algorithm will be validated for the solar concentrator system.

Data Availability

The data used to support the findings of this study are available from the corresponding author upon request.

Conflicts of Interest

The authors certify that they have no affiliations with or involvement in any organization or entity with any financial interest or nonfinancial interest in the subject matter or materials discussed in this manuscript.

Acknowledgments

The authors would like to thank Qatar University for granting the student grant (QUST-CENG-SPR\2017-23) which made this work possible. We would like to thank the Mechanical Engineering Department, Qatar University, for their assistance in designing the mechanical system.

References

- [1] W. E. Alnaser and N. W. Alnaser, "Solar and wind energy potential in GCC countries and some related projects," *Journal of Renewable and Sustainable Energy*, vol. 1, no. 2, article 022301, 2009.
- [2] I. Stamatescu, I. Făgărășan, G. Stamatescu, N. Arghira, and S. S. Iliescu, "Design and implementation of a solar-tracking algorithm," *Procedia Engineering*, vol. 69, pp. 500–507, 2014.
- [3] N. H. Helwa, A. B. G. Bahgat, A. M. R. El Shafee, and E. T. El Shenawy, "Maximum collectable solar energy by different solar tracking systems," *Energy Sources*, vol. 22, no. 1, pp. 23–34, 2000.
- [4] G. C. Lazaroiu, M. Longo, M. Roscia, and M. Pagano, "Comparative analysis of fixed and sun tracking low power PV systems considering energy consumption," *Energy Conversion and Management*, vol. 92, pp. 143–148, 2015.
- [5] C. S. Chin, A. Babu, and W. McBride, "Design, modeling and testing of a standalone single axis active solar tracker using MATLAB/Simulink," *Renewable Energy*, vol. 36, no. 11, pp. 3075–3090, 2011.
- [6] S. Ozcelik, H. Prakash, and R. Chaloo, "Two-axis solar tracker analysis and control for maximum power generation," *Procedia Computer Science*, vol. 6, pp. 457–462, 2011.
- [7] M. F. Werner, M. P. Woletz, and M. G. Zuzelski, "Single axis solar tracker," Canada Patent CA2889317A1, 2013.
- [8] R. G. Vieira, F. K. O. M. V. Guerra, M. R. B. G. Vale, and M. M. Araújo, "Comparative performance analysis between static solar panels and single-axis tracking system on a hot climate region near to the equator," *Renewable and Sustainable Energy Reviews*, vol. 64, pp. 672–681, 2016.
- [9] Y. Yao, Y. Hu, S. Gao, G. Yang, and J. Du, "A multipurpose dual-axis solar tracker with two tracking strategies," *Renewable Energy*, vol. 72, pp. 88–98, 2014.
- [10] M. Neber, H. Lee, L. Barker, C. G. Olaes, D. Marumoto, and J. Valdez, "Two-axis solar tracker design for low cost deployment and profile for reduced loading moments," US Patents 9-093587, 2015.
- [11] S. J. Oh, M. Burhan, K. C. Ng, Y. Kim, and W. Chun, "Development and performance analysis of a two-axis solar tracker for concentrated photovoltaics," *International Journal of Energy Research*, vol. 39, no. 7, pp. 965–976, 2015.
- [12] K. Maharaja, R. J. Xavier, L. J. Amla, and P. P. Balaji, "Intensity based dual axis solar tracking system," *International Journal of Applied Engineering Research*, vol. 10, no. 8, pp. 19457–19465, 2015.
- [13] H. Fathabadi, "Novel high efficient offline sensorless dual-axis solar tracker for using in photovoltaic systems and solar concentrators," *Renewable Energy*, vol. 95, pp. 485–494, 2016.
- [14] B. Muhammad, J. O. Seung, K. C. Ng, and W. Chun, "Experimental investigation of multijunction solar cell using two axis solar tracker," *Applied Mechanics and Materials*, vol. 818, pp. 213–218, 2016.
- [15] L. Barker, M. Neber, and H. Lee, "Design of a low-profile two-axis solar tracker," *Solar Energy*, vol. 97, pp. 569–576, 2013.
- [16] H. Fathabadi, "Novel high accurate sensorless dual-axis solar tracking system controlled by maximum power point tracking unit of photovoltaic systems," *Applied Energy*, vol. 173, pp. 448–459, 2016.
- [17] D. Verma, S. Nema, A. M. Shandilya, and S. K. Dash, "Maximum power point tracking (MPPT) techniques: recapitulation in solar photovoltaic systems," *Renewable and Sustainable Energy Reviews*, vol. 54, pp. 1018–1034, 2016.
- [18] D. C. Huynh and M. W. Dunnigan, "Development and comparison of an improved incremental conductance algorithm for tracking the MPP of a solar PV panel," *IEEE Transactions on Sustainable Energy*, vol. 7, no. 4, pp. 1421–1429, 2016.
- [19] N. Pellet, F. Giordano, M. Ibrahim Dar et al., "Hill climbing hysteresis of perovskite-based solar cells: a maximum power point tracking investigation," *Progress in Photovoltaics: Research and Applications*, vol. 25, no. 11, pp. 942–950, 2017.

- [20] N. Parmar, A. N. Parmar, and V. S. Gautam, "Passive solar tracking system," *International Journal of Emerging Technology and Advanced Engineering*, vol. 5, no. 1, pp. 138–145, 2015.
- [21] H. Jiang, C. Li, and Y. Liu, "Passive solar tracking system to enhance solar cell output," US Patents 9-548697, 2017.
- [22] Z. Mi, J. Chen, N. Chen, Y. Bai, R. Fu, and H. Liu, "Open-loop solar tracking strategy for high concentrating photovoltaic systems using variable tracking frequency," *Energy Conversion and Management*, vol. 117, pp. 142–149, 2016.
- [23] C.-K. Yang, T. C. Cheng, C. H. Cheng, C. C. Wang, and C. C. Lee, "Open-loop altitude-azimuth concentrated solar tracking system for solar-thermal applications," *Solar Energy*, vol. 147, pp. 52–60, 2017.
- [24] C. Alexandru, "A novel open-loop tracking strategy for photovoltaic systems," *The Scientific World Journal*, vol. 2013, 12 pages, 2013.
- [25] Z. Liu, B. Wang, and W. Tong, "High precision dual-axis tracking solar wireless charging system based on the four quadrant photoelectric sensor," in *2015 International Conference on Optical Instruments and Technology: Optoelectronic Measurement Technology and Systems*, Beijing, China, August 2015.
- [26] K. Azizi and A. Ghaffari, "Design and manufacturing of a high-precision sun tracking system based on image processing," *International Journal of Photoenergy*, vol. 2013, 7 pages, 2013.
- [27] F. Wang, X.-q. Zhang, and H. Meng, "High precision automatic tracking system based on photosensitive resistance," *Electro-Optic Technology Application*, vol. 5, p. 5, 2015.
- [28] J. Huang, K. Deng, D. Jiang, P. Zhang, B. Zhu, and Z. Yao, "Analysis for image contrast of extended objects in photoelectric tracking system," *Electronics Optics & Control*, vol. 5, p. 4, 2015.
- [29] J.-M. Wang and C.-L. Lu, "Design and implementation of a sun tracker with a dual-axis single motor for an optical sensor-based photovoltaic system," *Sensors*, vol. 13, no. 3, pp. 3157–3168, 2013.
- [30] A. G. Melo, D. Oliveira Filho, M. M. Oliveira Junior, S. Zolnier, and A. Ribeiro, "Development of a closed and open loop solar tracker technology," *Acta Scientiarum*, vol. 39, no. 2, p. 177, 2017.
- [31] C.-C. Wei, Y.-C. Song, C.-B. Lin, and L. Chiang, "Design of a sun tracking system based on the brightest point in sky image," in *2016 Third International Conference on Computing Measurement Control and Sensor Network (CMCSN)*, Matsue, Japan, May 2016.
- [32] C.-H. Tsai, S. C. Hu, C. H. Huang, and Y. C. Tseng, "A sensor-based sun-tracking energy harvest system," *International Journal of Sensor Networks*, vol. 19, no. 2, pp. 104–113, 2015.
- [33] I. J. Gabe, A. Bühler, D. Chesini, and F. Frosi, "Design and implementation of a low-cost dual-axes autonomous solar tracker," in *2017 IEEE 8th International Symposium on Power Electronics for Distributed Generation Systems (PEDG)*, Florianopolis, Brazil, April 2017.
- [34] I. Reda and A. Andreas, "Solar position algorithm for solar radiation applications," *Solar Energy*, vol. 76, no. 5, pp. 577–589, 2004.
- [35] J. J. Michalsky, "The Astronomical Almanac's algorithm for approximate solar position (1950–2050)," *Solar Energy*, vol. 40, no. 3, pp. 227–235, 1988.
- [36] R. Grena, "An algorithm for the computation of the solar position," *Solar Energy*, vol. 82, no. 5, pp. 462–470, 2008.
- [37] H. Fathabadi, "Comparative study between two novel sensorless and sensor based dual-axis solar trackers," *Solar Energy*, vol. 138, pp. 67–76, 2016.
- [38] R. N. Syafii and M. Hadi, "Improve dual axis solar tracker algorithm based on sunrise and sunset position," *Journal of Electrical Systems*, vol. 11, no. 4, 2015.

